

MicroRNA-140-5p inhibits tumor growth and metastasis by targeting FGF9 in colorectal cancer

Xueyong Zhang¹, Chenghui Zhou², Juan Wu³ and Hao Yang^{2,4}

¹Department of Ophthalmology, Xiangya Hospital, Central South University, Changsha, Hunan, P.R. China 410008

²Department of Geriatric Surgery, Xiangya Hospital, Central South University, Changsha, Hunan, P.R. China 410008

³Department of Geriatrics, Xiangya Hospital, Central South University, Changsha, Hunan, P.R. China 410008

⁴National Clinical Research Center for Geriatric Disorders, Xiangya Hospital, Central South University, Changsha, Hunan, P.R. China 410008

Correspondence to: Hao Yang, **email:** yh727888@126.com

Keywords: miR-140-5p; FGF9; metastasis; prognosis; colorectal cancer

Received: May 23, 2018

Accepted: July 31, 2018

Published:

Copyright: Zhang et al. This is an open-access article distributed under the terms of the Creative Commons Attribution License 3.0 (CC BY 3.0), which permits unrestricted use, distribution, and reproduction in any medium, provided the original author and source are credited.

ABSTRACT

Background and aims: The aberrant expression of miR-140-5p has been described in colorectal cancer (CRC). However, considering that various protein coding genes are targeted by one miRNA, the role of miR-140-5p in CRC remains unclear. In this study, the biological function and prognostic relevance of miR-140-5p in CRC was investigated.

Methods: miR-140-5p level was determined in 100 paired fresh specimens through quantitative real-time PCR. FGF9 as the target of miR-140-5p was verified through a dual luciferase reporter assay, and the effects of miR-140-5p and FGF9 on phenotypic changes in CRC cells were investigated *in vitro* and *in vivo*.

Results: Compared with that in adjacent normal tissues, miR-140-5p expression decreased in cancerous tissues. The down-regulated miR-140-5p in 100 patients with CRC was significantly correlated with the reduced overall survival of these patients. miR-140-5p inhibits CRC cell proliferation, migration and invasion by targeting FGF9.

Conclusions: miR-140-5p serves as a potential prognostic factor in patients with CRC. FGF9 regulated by miR-140-5p is a novel mechanism behind the promoting effects of FGF9 in CRC.

INTRODUCTION

Colorectal cancer (CRC) is one of the most common human cancers in the world. It ranks as the third most commonly diagnosed cancer in males and the second in females, with an estimated 1.4 million cases and 693,900 deaths occurring in 2012 [1]. In recent years, decreasing colorectal cancer mortality rates have been observed in a large number of countries worldwide and are most likely attributed to colorectal cancer screening, reduced prevalence of risk factors, and/or improved treatments [2, 3]. However, its long-term prognosis remains unsatisfactory, mainly due to the high recurrence and metastasis rate [4]. It has been generally accepted that the

invasive and metastatic potentials of cancer are mostly attributed to the differences of pathological and molecular characteristics [5]. However, the molecular mechanisms for CRC development and prognosis are still unclear.

MicroRNAs (miRNAs) are a class of small, endogenously expressed, well-conserved noncoding RNA molecules with 18–25 nucleotides (nt). They play important regulatory roles by targeting mRNAs for cleavage or translational repression [6]. Given that more than 50% of miRNAs are located in cancer-associated genomic regions or in fragile sites, miRNAs may play an important role in cancer pathogenesis [7]. Indeed, aberrant miRNA expression has been demonstrated in CRC, which contributes to carcinogenesis and cancer development

by promoting oncogene expression or by inhibiting tumor suppressor genes [8–11]. Expression profiling of tumors and normal tissues has revealed a possible tumor suppressive role for miR-140-5p in many cancers, including ovarian cancer [12], lung cancer [13, 14], CRC [15, 16], osteosarcoma [15], hepatocellular carcinoma [17], breast cancer [18], esophageal cancer [19] and basal cell carcinoma [20]. Although miR-140-5p is generally accepted as a tumor suppressor, an oncogenic role of miR-140-5p has also been implicated depending on different cell context [21–24]. Based on these many controversial issues and considering that various protein coding genes are targeted by one miRNA, the precise mechanism of miR-140-5p in CRC still need to be further investigated.

This study was to examine the effects and mechanism of miR-140-5p on the migration and invasion

of CRC and to evaluate the miR-140-5p expression and its prognosis value CRC patients.

RESULTS

miR-140-5p is down-regulated in CRC cell lines and tissues

To study expression of miR-140-5p in CRC cells and tissues, real-time polymerase chain reaction (PCR) were performed. 100 pairs of CRCs and corresponding ANCMTs were used here. miR-140-5p expression in CRC tissues was markedly lower than ANCMTs (Figure 1A). Comparing samples with metastasis to nonmetastasis samples, metastasis samples have the lower expression of miR-140-5p (Figure 1B). Then, expression of miR-140-5p

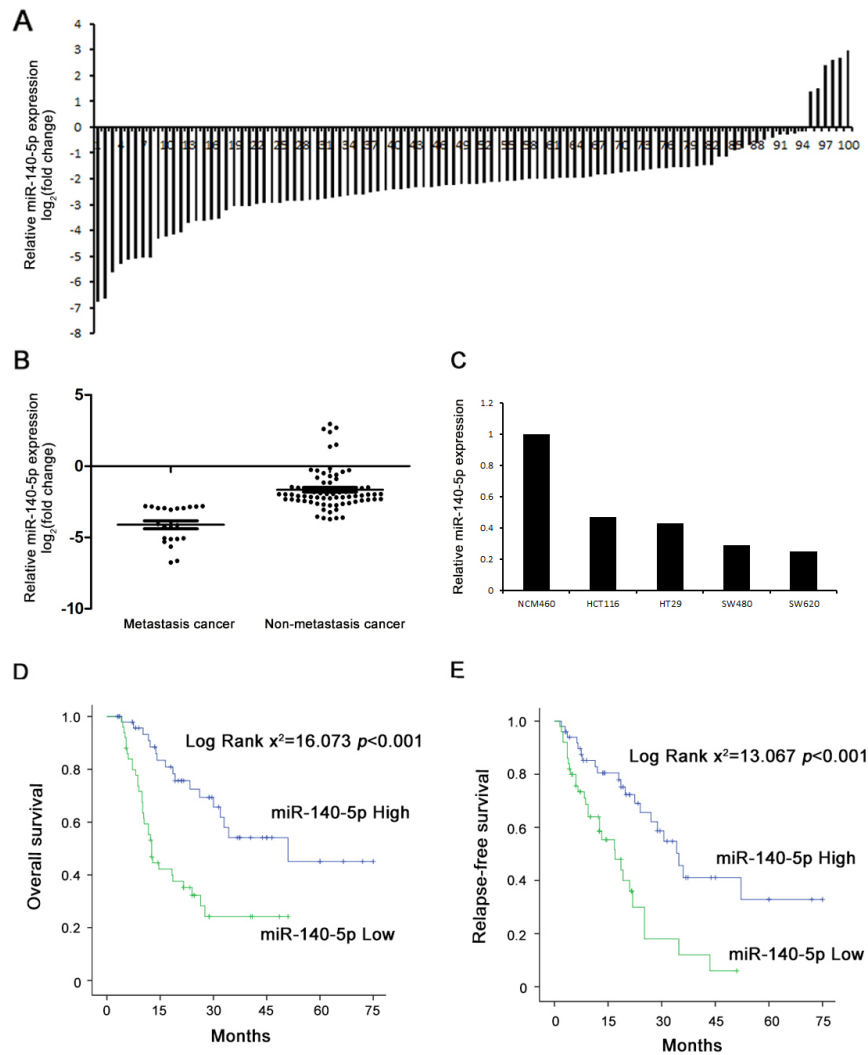


Figure 1: miR-140-5p expression is down-regulated in CRC and indicates poor prognosis. (A and C) Real-time PCR showed the expression of miR-140-5p is down-regulated in human CRC tumor tissues and cell lines. (B) miR-140-5p is down-regulated in metastasis cancer tissues. (D and E) OS and RFS of CRC patients with high or low miR-140-5p expression. Survival curve was calculated with the log-rank test.

Table 1: Correlations between miR-140-5p expression level and clinicopathological variables of 100 cases of CRC

Clinicopathologic variables	miR-140-5p expression			P Value
	n	Low	High	
Gender				
Male	69	38	31	
Female	31	12	19	0.133
Age(years)				
≤60	66	30	36	
>60	34	20	14	0.209
Histological grade				
Well and moderate	18	5	13	
Poor and other	82	45	37	0.038
T stage				
T1-T2	41	17	24	
T3-T4	59	33	26	0.158
Lymph node metastasis				
Presence	53	28	25	
Absence	47	22	25	0.552
TNM stage				
I-II	35	21	14	
III-IV	65	29	36	0.145

in CRC cells and human normal colorectal cell line were also detected. Compared with NCM460 cells, which are immortalized human normal colorectal cell line, miR-140-5p was low-expressed in CRC cells (Figure 1C), which is consistent with the decreased miR-140-5p expression in CRC tissues. These data indicated that miR-140-5p was down-regulated in CRCs and it might be correlated with CRC invasion and metastasis.

Low miR-140-5p expression is associated with poor CRC clinicopathological features and shorter survival

We then estimated the association of miR-140-5p expression with clinicopathological features and survival of CRC patients. Our results showed that a low expression level of miR-140-5p was significantly associated with histological grade (Table 1). CRC patients in the low miR-140-5p expression group had shorter OS (Log Rank $X^2=16.073$, $p < 0.001$) and RFS rates (Log Rank $X^2=13.067$, $p < 0.001$) than patients in the high-expression group (Figure 1D and 1E). Furthermore, univariate and multivariate analysis revealed that histological grade, lymph node metastasis, TNM stage and low miR-140-5p expression were independent risk factors for OS and

lymph node metastasis, TNM stage and low miR-140-5p expression were independent risk factors for RFS of CRC patients after colorectal resection (Table 2 and Table 3). These results fully demonstrated that miR-140-5p was closely correlated with poor survival and could be used as a novel independent prognosis biomarker for CRC patients after colorectal resection.

miR-140-5p suppresses CRC cell proliferation, migration and invasion

To understand the function of miR-140-5P in CRC cells, we manipulated miR-140-5P expression in cells by ectopic expression and anti-miR-140-5p expression lentivirus. Ectopic miR-140-5P was constitutively expressed in SW480 and SW620 cells named as SW480-miR-140-5P and SW620-miR-140-5p subsequently. Meanwhile, anti-miR-140-5p lentivirus was designed to silence miR-140-5P expression in HCT116 cells named as HCT116-anti-miR-140-5P subsequently. Expression level of miR-140-5P was identified by real-time PCR (Figure 2A). We performed cell cycle analysis and revealed that miR-140-5p arrested the cells at G1 phase. Ectopic miR-140-5p expression decreased the percentage of cells in G1 phase from 58% to 41% ($P < 0.05$) in SW480 cells

Table 2: The Cox regression analyses of overall survival (OS) and miR-140-5p expression level as well as clinicopathological parameters

Variables	Univariable analysis			Multivariable analysis	
	n	HR (95% CI)	P	HR (95% CI)	P
Gender					
Male	69	1			
Female	31	0.58 (0.31-1.09)	0.093	0.54 (0.27-1.09)	0.088
Age(years)					
≤60	66	1			
>60	34	1.44(0.82-2.51)	0.203	NA	NA
Histological grade					
Well and moderate	18	1		1	
Poor and other	82	2.01(1.07-3.77)	0.031	2.16(1.12-4.20)	0.022
T stage					
T1-T2	41	1			
T3-T4	59	1.12 (0.64-1.96)	0.703	NA	NA
Lymph node metastasis					
Presence	53	1		1	
Absence	47	0.41 (0.23-0.72)	0.002	0.39 (0.21 -0.74)	0.004
TNM stage					
I-II	35	1		1	
III-IV	65	3.15 (1.79-5.56)	<0.001	2.54(1.36-4.77)	0.004
miR-140-5p expression					
High	50	1		1	
Low	50	3.19 (1.76-5.79)	<0.001	2.96 (1.58-5.54)	0.001

and from 61% to 41% ($P < 0.05$) in SW620 cells, but increased the percentage of cells in S phase phase from 37% to 48% ($P < 0.05$) in SW480 cells and from 35% to 49% ($P < 0.05$) in SW620 cells, respectively (Figure 2B). Compared to SW480 and SW620, SW480- miR-140-5P and SW620-miR-140-5p had lower proliferation rate (Figure 2C). Consistently, SW480- miR-140-5P and SW620-miR-140-5p cells also formed fewer colonies in colony formation assay (Figure 2D). In contrast, HCT116-anti-miR-140-5P cells had increased cell proliferation rate and clonogenicity capacity (Figure 2C, 2D). The wound-healing and transwell assays were used to investigate migration and invasion capacity. Results showed that SW480- miR-140-5P and SW620-miR-140-5p cells had lower wound closure rate and more invasion cells than SW480 cells and SW620 cells, whereas HCT116-anti-miR-140-5P cells had markedly increased migratory and invasive capacity (Figure 2E, 2F). It suggests that miR-140-5P suppresses CRC cell proliferation, migration, and invasion capacity.

FGF9 is targeted by miR-140-5p in colorectal cancer

Our previous study had showed that miR-140-5p suppressed tumor growth and metastasis by targeting MIR-140-5P in Hepatocellular carcinoma [17]. Therefore, we speculated that miR-140-5p might have the same effect in colorectal cancer. Firstly, we detected the expression of FGF9 in CRC cells and tissues. Our data showed that FGF9 is significantly up-regulated in CRC tissues (Figure 3A). And then, we constructed luciferase reporter assay system to detect whether miR-140-5p could binds to the 3'-UTR of FGF9 (Figure 3B). Our data showed that miR-140-5p remarkably reduced the wild type FGF9 luciferase activity, whereas cells with mutant FGF9 3'-UTR displayed much higher luciferase activity (Figure 3C). Finally, we used western blotting analysis to further demonstrate that ectopic miR-140-5p dramatically suppressed the endogenous protein levels for FGF9 in SW-480 cells (Figure 3D).

Table 3: The Cox regression analyses of disease-free survival (DFS) and miR-140-5p expression level as well as clinicopathological parameters

Variables	Univariable analysis			Multivariable analysis	
	n	HR (95% CI)	P	HR (95% CI)	P
Gender					
Male	69	1			
Female	31	0.60 (0.32-1.11)	0.104	NA	NA
Age(years)					
≤60	66	1			
>60	34	0.93(0.52-1.68)	0.809	NA	NA
Histological grade					
Well and moderate	18	1			
Poor and other	82	1.34(0.67-2.68)	0.408	NA	NA
T stage					
T1-T2	41	1			
T3-T4	59	1.20 (0.68-2.12)	0.533	NA	NA
Lymph node metastasis					
Presence	53	1		1	
Absence	47	0.54 (0.30-0.95)	0.033	0.55 (0.30 -0.99)	0.046
TNM stage					
I-II	35	1		1	
III-IV	65	2.69 (1.48-4.91)	0.001	2.22(1.19-4.13)	0.012
miR-140-5p expression					
High	50	1		1	
Low	50	2.84 (1.57-5.11)	0.001	2.79 (1.54-5.08)	0.001

Ectopic miR-140-5p expression in FGF9 transduced cells attenuated the effect of FGF9 on CRC growth and metastasis

Then, we want to further confirm the effect of miR-140-5p on invasion, metastasis and growth of colorectal cancer is through by targeting FGF9. Therefore, we transduced ectopic FGF9 into miR-140-5p transduced SW480 cells by FGF9 lentiviral expression vector. We detected the expression of FGF9 by real-time PCR (Figure 4A). We found that ectopic FGF9 expression in miR-140-5p transduced cells attenuated the inhibitory effect of miR-140-5p on CRC growth and metastasis (Figure 4B-4F). Taken together, our data suggest that MiR-140-5P may inhibit tumor growth and metastasis by targeting FGF9 in CRC.

DISCUSSION

Invasion and metastasis are responsible for the vast majority of cancer associated deaths [25]. Mounting

studies have indicated that miRNAs can play crucial roles in epigenetic regulation of tumor-related gene expression and could act as an effective biomarker for the tumor diagnosis, prognosis or even therapy [26–28]. It has been reported that miR-140-5p play an important role in cellular function, including growth, invasion, metastasis and EMT [13, 17, 19, 29]. The aberrant expression of miR-140-5p is a frequent event in various kinds of cancers, suggesting an important role for miR-140-5p in the tumor initiation and progression [13, 17, 19, 29].

However, the molecular significance and the role in CRC metastasis of miR-140-5p are still elusive. In the current study, we used qRT-PCR to show that miR-140-5p levels in colorectal cancer tissues were significantly lower than those in non-tumor tissues. Moreover, the miR-140-5p levels were associated with histological grade. Kaplan–Meier survival analysis revealed that patients whose primary tumors displayed low expression of miR-140-5p had shorter OS and RFS in CRC. In addition, Cox proportional hazards regression analysis showed

that decreased miR-140-5p in tumors was a strong and independent predictor of shorter OS and RFS. The results derived from *in vitro* cell proliferation, colony formation, migration, invasion assays also showed that ectopic miR-140-5p expression inhibits the potency for CRC cell proliferation and metastasis, while blocked miR-140-5p expression showed the opposite effect. Next, we used luciferase reporter assay, western blot analysis to prove that FGF9 is the target gene of miR-140-5p in CRC. Moreover, our data showed that reintroduction of FGF9

could partly abolish the effect of miR-140-5p on CRC. Our findings also suggest that miR-140-5p could potentially be used as a biomarker to clinically predict metastasis and survival prognosis for the patients with CRC.

In conclusion, miR-140-5p is down-regulated in CRC and possesses the potency to suppress CRC growth and metastasis which are through targeted FGF9. Therefore, miR-140-5p could function as a tumor suppressor in CRC. The identification the role of miR-140-5p/FGF9 in CRC would help in better understanding of

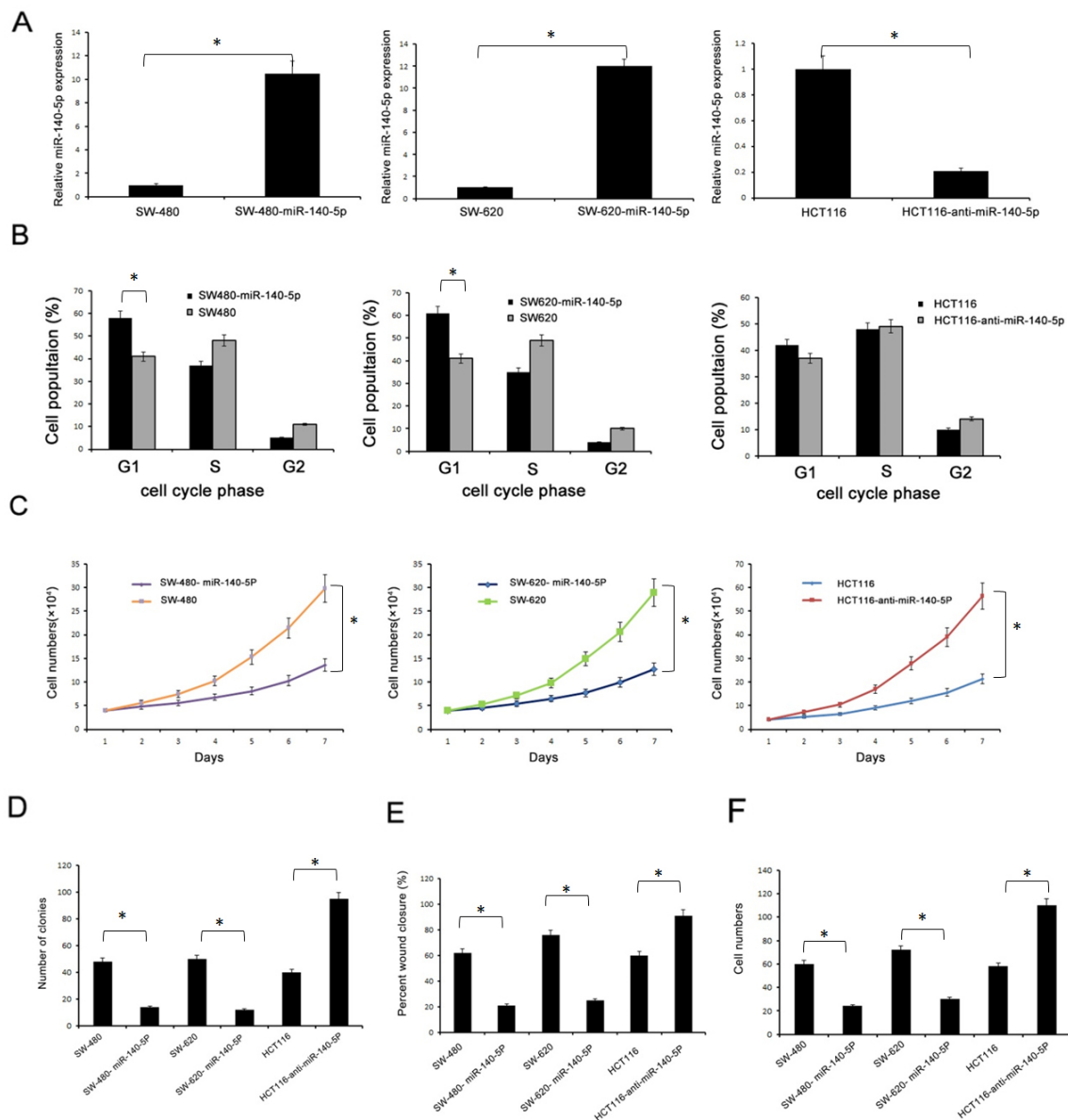


Figure 2: miR-140-5p inhibits proliferation and metastasis of CRC *in vitro*. (A) Expression level of miR-140-5p was identified by real-time PCR in SW480, SW480-miR-140-5p, SW620, SW620-miR-140-5p, HCT116 and HCT116-anti-miR-140-5p cells. (B) The cell cycle distribution of SW480, SW620, HCT116 cells infected with miR-140-5p lentivirus or control vector were analyzed as described in Materials and Methods. (C and D) Proliferation of SW480-miR-140-5p, HCT116-anti-miR-140-5p cells and control cells was examined by cell proliferation and colony formation assays. (E) Wound-healing assay and (F) transwell invasion assay were subjected to detect the migration and invasion capacity of miR-140-5p-interfered cells. * $P < 0.05$ based on the Student *t* test.

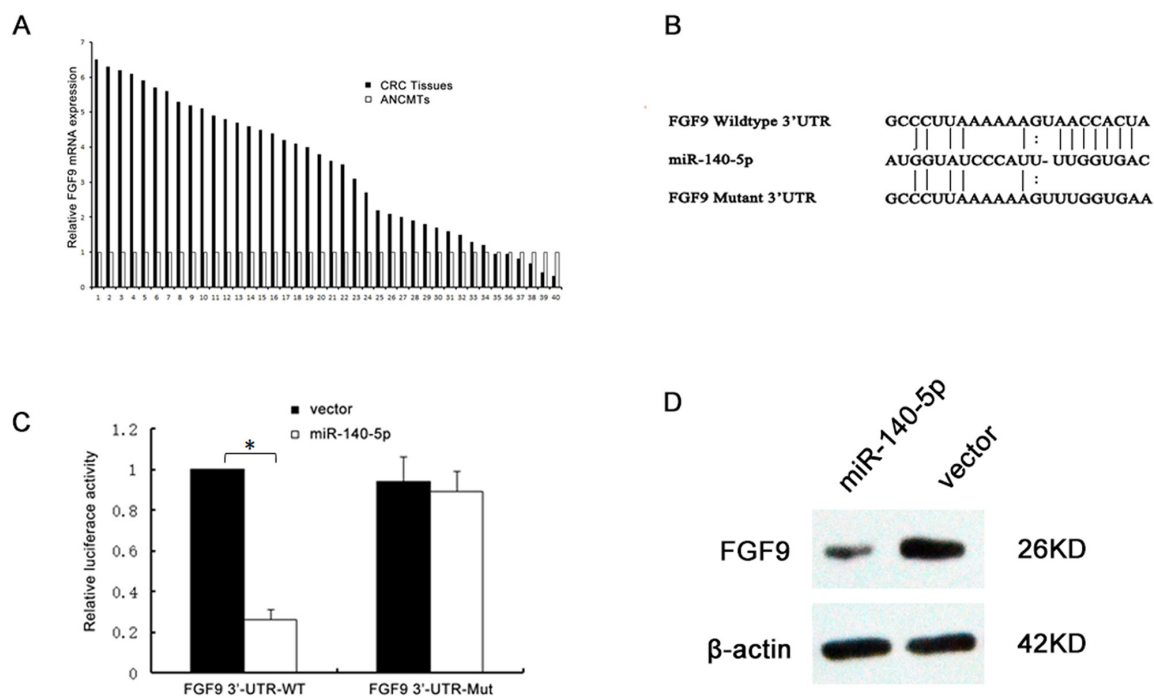


Figure 3: FGF9 are direct downstream targets for miR-140-5p. (A) The expression levels of FGF9 in CRC and ANCMTs were analyzed by real-time PCR. (B) miR-140-5p and its putative binding sequence in the 3'-UTR of FGF9. The mutant miR-140-5p-binding site was generated in the complementary site for the seed region of miR-140-5p. (C) Relative luciferase activity was analyzed. HEK293T cells were cotransfected with pGL3 (vector) or pGL3-miR-140-5p, firefly luciferase reporter containing either a wildtype or a mutant 3'-UTR (indicated as WT or Mut on the X axis), and a Renilla luciferase expressing construct (as internal control to calibrate the differences in both transfection and harvest efficiencies). The firefly luciferase activity of each sample was normalized to the Renilla luciferase activity. The normalized luciferase activity of wildtype pGL3-transfectants in each experiment was set as relative luciferase activity. (D) Western blot results of endogenous FGF9 proteins in HEK293T cells infected with miR-140-5p lentivirus or vector control. * $P < 0.05$ based on the Student t test.

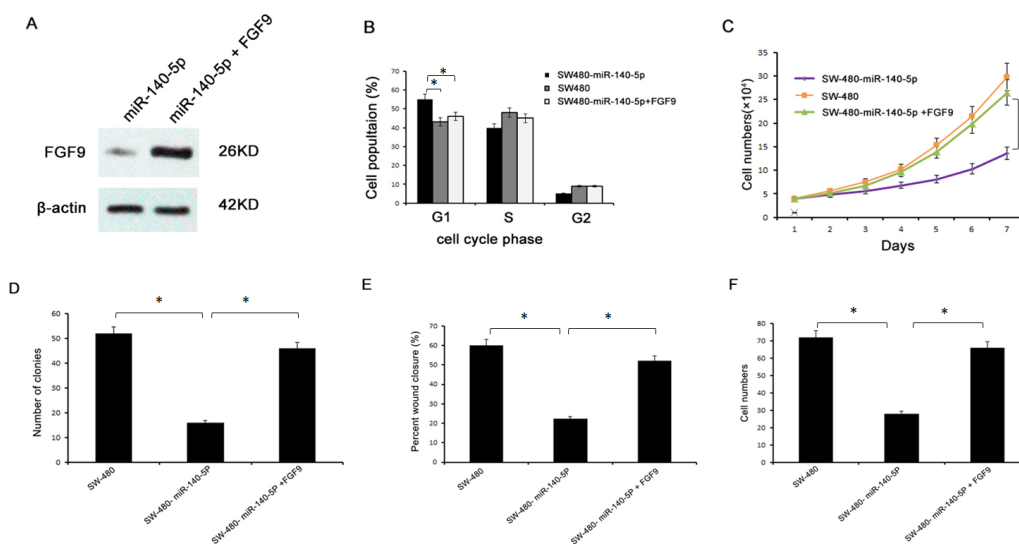


Figure 4: Both gain- and loss-of-function studies showed that FGF9 abrogates the suppressive roles of miR-140-5p in CRC cell proliferation, migration and invasion. (A) Expression level of FGF9 was identified by western blot in SW480-miR-140-5p and SW480-miR-140-5p + FGF9 cells. (B) Cell cycle distribution assay was performed to detect the cell cycle of above cells. (C and D) Proliferation of SW-480, SW-480-miR-140-5p and SW-480-miR-140-5p + FGF9 cells was examined by cell proliferation and colony formation assays. (E) Wound-healing assay and (F) transwell invasion assay were subjected to detect the migration and invasion capacity of FGF9-interfered cells. * $P < 0.05$ based on the Student t test.

the molecular mechanisms underlying CRC development, which would provide us a wider prospective on CRC intervention/prevention and treatment.

MATERIALS AND METHODS

A total of 100 pairs of fresh CRCs and adjacent nontumor colorectal mucosa tissues (ANCMTs) obtained from consecutive patients who have received colorectal resection for CRC at the Department of Geriatric Surgery, Xiangya Hospital of Central South University (CSU) from January 2010 to October 2010. Diagnosis of CRC was confirmed by two independent histopathologists. In total 78 males and 22 females with a median age of 47.5 years (range: 20-81) were included for the study. The related clinicopathological characteristics of these samples are presented in the Table 1. Prior informed consent was obtained and the study protocol was approved by the Ethics Committee of Xiangya Hospital of CSU.

Cell Lines and Cell Culture. Human CRC cell lines SW620, SW480, HT29, HCT116 cells were purchased from the cell bank of the Chinese Academy of Sciences (Shanghai, China). NCM460 cell was purchased from American INCELL Corporation. These cells were cultured in High glucose Dulbecco's modified Eagle media (GIBCO BRL, Gaithersburg, MD, USA) supplemented with 10% fetal bovine serum (HyClone, Logan, UT, USA) and 5% CO₂ at 37°C.

Quantitative Real-time Quantitative PCR (qRT-PCR). qRT-PCR was performed using TaqMan® Universal PCR Master Mix (Ambion, TX, USA) and TaqMan® MicroRNA reverse transcription kit as instructed. Real time RT-PCR was performed using a PRISM 7300 Sequence Detection System (Applied Biosystems, CA, USA), in which each reaction (25 ul) contained 10ul PCR Master Mix (Ambion, TX,) and 1.33ul RT product, and each sample was analyzed in triplicates. PCR was carried out at 95°C for 10 min, followed by 40 cycles of amplification at 95°C for 15 s and 60°C for 60 s. Results are representative of two independent assays. Relative fold changes of expression in tumor tissues against nontumor samples and among different cell lines were calculated using the comparative Ct ($2^{-\Delta\Delta Ct}$) method with U6 small nuclear RNA (Ambion, TX, USA) as the endogenous control.

Western Blotting analysis. Total proteins were extracted and separated by sodium dodecyl sulfate-polyacrylamide gel electrophoresis (SDS-PAGE) and then transferred onto PVDF membrane (Millipore, Bedford, MA, USA). The blotted membranes were incubated with antihuman FGF9 antibody (1:1000, Santa Cruz Biotechnology, Santa Cruz, CA, USA), and then probed with a secondary antibody (1:3000, Santa Cruz Biotechnology) Beta-actin was used as a loading control.

Immunohistochemistry. Formalin-fixed paraffin sections were stained for FGF9 using the streptavidin-peroxidase system (Zhong-shan Goldenbridge

Biotechnology, Beijing, China). Negative control slides were probed with goat serum followed by the secondary antibody under the same conditions. The expression levels of FGF9 were scored using a 4-point scale according to the percentage of positive gastric cell: 0, ≤10% positive; 1+, 11% to 25% positive; 2+, 26% to 50% positive; 3+, ≥51% positive. The protein expression of FGF9 was thus considered negative if scored 0 or 1+ and 2+ or 3+ were considered positive.

Follow-up and Prognostic Study. Follow-up data were obtained after colorectal resection for all 100 patients. The average observation time for overall survival and disease-free survival were 40 months (10 to 84 months) and 31 months (8.5 to 84 months), respectively. Among all patients analyzed, 31 of which were died during the follow-up period, while 42 patients were found with tumor recurrence. The follow-up period was defined as the interval between the date of operation and the deadline (December 2017). Recurrence and metastasis were diagnosed by clinical examination, colonoscopy, ultrasonography and computed tomography (CT) scan. To determine factors influencing survival after colorectal resection, 7 conventional variables were tested in all 100 patients, which include gender, age, histological grade, T stage, lymph node metastasis, TNM stage and miR-140-5p expression levels.

Vector Construction and Cell Transfection. The DNA fragment for miR-140-5p was amplified from genomic DNA and inserted into the Age I/EcoR I site of a lentiviral expression vector pCRCSIL-GFP (GeneChem, Shanghai, China). The FGF9 expression vector were constructed by inserting their ORF sequence into the pCRCL vector (GeneChem, Shanghai, China). Cell transfection was performed according to the protocol of manufactures. Viruses were harvested 72 hours after transfection and viral titers were determined (1×10^9 TU/ml). 1×10^5 cells were infected with 2×10^6 lentivirus in the presence of 6ug/ml polybrene (Sigma, MO). In the present study, the infection efficiency of lentivirus was over 90%. There were no significant cell death been observed after virus infection, and bulk transfectants were used for subsequent assays. For luciferase analysis, the 3'-UTR sequence of FGF9 were amplified from human stomach genomic DNA and then cloned into the downstream region of a firefly luciferase cassette in the pGL3-Promoter vector (Promega, Madison, WI, USA) as instructed.

Cell cycle analysis. 5×10^5 cells were seeded in 6-well plates and incubated for 24 h. Then cells were harvested and fixed with cold 70% ethanol at -20°C overnight. After washing, cells were stained in a solution containing PI (0.5 mg/mL) and RNase A (10 mg/mL). Then cells were filtered through a 70 μM cell strainer immediately prior to flow cytometry, which was carried out on a FACS caliber flow cytometer (BD Biosciences, San Jose, CA, USA).

Cell Proliferation and Colony Formation Assays. Cell proliferation was determined by counting the number

of cells using TC10™ automated cell counter (Bio Rad, CA). For colony formation assays, 500 cells were seeded into 35mm dishes (Corning, NY) and cultured for 2 weeks at 37°C. The numbers of colonies per dish were counted after staining with crystal violet. All studies were conducted with 3 replicates.

In Vitro Wound Healing (Migration) and Invasion Assays. Cells were seeded onto 35mm dishes coated with fibronectin. After the cells reached 100% confluence, wound healing assays were performed with a sterile pipette tip to make a scratch through the confluent monolayer. Medium was changed and the cells were cultured for another 48 hours. The percent of wound closure was calculated for five randomly chosen fields. For the invasion assay, 1×10^5 cells in serum-free medium containing 0.1% bovine serum albumin were placed into the upper chamber of the insert with Matrigel (BD Biosciences, MA). After 64 hours of incubation at 37°C, the cells remained in the upper chamber or on the upper membrane were removed. The number of cells adhering to the lower membrane of the inserts was counted after staining with a solution containing 0.1% crystal violet and 20% methanol.

Luciferase Reporter Assay. Luciferase activity was assessed according to the Dual-Luciferase Reporter Assay protocol (Promega, Madison, WI) using a Veritas™ 96-well Microplate Luminometer (Promega, Madison, WI) with substrate dispenser (Promega, Madison, WI). HEK293T cells transduced with leti-miR-140-5p or control virus were seeded in 96-well plates with 70% confluence. 12 hours later, the cells were cotransfected with 50 ng pGL3-UTR and 10 ng pRLTK using the Lipofectamine LTX. After 24 hours of transfection, the cells were harvested for firefly and Renilla luciferase activity assay. The renilla luciferase activities were used to normalize the transfection efficiency.

Statistical analysis. Statistical analysis was performed using the SPSS (version 13.0, Chicago, IL, USA). Data for miR-140-5p expression in fresh specimens were analyzed using the Mann–Whitney U-test. Fisher's exact test was used for statistical analysis of categorical data. Spearman correlation test was used for analyzing the correlations between miR-140-5p expression level and the clinical and pathological variables. Survival curves were constructed using the Kaplan–Meier method and evaluated using the log-rank test. The cox proportional hazard regression model was used to identify factors that were independently associated with overall survival and disease-free survival. In any case, $P < 0.05$ was considered with statistical significance.

Abbreviations

FGF9, fibroblast growth factor 9; miR-140-5p, microRNA-140-5p; ANCMT, adjacent nontumorous colorectal mucosa tissue; CRT, colorectal tumor; qRT-PCR, Real-time quantitative PCR.

CONFLICTS OF INTEREST

The authors have declared that no conflicts of interest exists.

GRANT SUPPORT

National Nature Science Foundation of China (No. 81502539). Nature Science Foundation of Xiangya (No. 2013Q07).

INFORMED CONSENT

Prior informed consent was obtained from all the individuals involved in this study.

REFERENCES

1. Torre LA, Bray F, Siegel RL, Ferlay J, Lortet-Tieulent J, Jemal A. Global cancer statistics, 2012. *CA Cancer J Clin*. 2015; 65: 87–108.
2. Edwards BK, Ward E, Kohler BA, Ehemann C, Zauber AG, Anderson RN, Jemal A, Schymura MJ, Lansdorp-Vogelaar I, Seeff LC, van Ballegooijen M, Goede SL, Ries LA. Annual report to the nation on the status of cancer, 1975-2006, featuring colorectal cancer trends and impact of interventions (risk factors, screening, and treatment) to reduce future rates. *Cancer*. 2010; 116: 544–73.
3. Bosetti C, Levi F, Rosato V, Bertuccio P, Lucchini F, Negri E, La Vecchia C. Recent trends in colorectal cancer mortality in Europe. *Int J Cancer*. 2011; 129: 180–91.
4. Hegde SR, Sun W, Lynch JP. Systemic and targeted therapy for advanced colon cancer. *Expert Rev Gastroenterol Hepatol*. 2008; 2: 135–49.
5. Grady WM, Markowitz SD. The molecular pathogenesis of colorectal cancer and its potential application to colorectal cancer screening. *Dig Dis Sci*. 2015; 60: 762–72.
6. Bartel DP. MicroRNAs: genomics, biogenesis, mechanism, and function. *Cell*. 2004; 116: 281–97.
7. Calin GA, Sevignani C, Dumitru CD, Hyslop T, Noch E, Yendamuri S, Shimizu M, Rattan S, Bullrich F, Negrini M, Croce CM. Human microRNA genes are frequently located at fragile sites and genomic regions involved in cancers. *Proc Natl Acad Sci U S A*. 2004; 101: 2999–3004.
8. Dong Y, Wu WK, Wu CW, Sung JJ, Yu J, Ng SS. MicroRNA dysregulation in colorectal cancer: a clinical perspective. *Br J Cancer*. 2011; 104: 893–8.
9. Bonfrate L, Altomare DF, Di Lena M, Travaglio E, Rotelli MT, De Luca A, Portincasa P. MicroRNA in colorectal cancer: new perspectives for diagnosis, prognosis and treatment. *J Gastrointest Liver Dis*. 2013; 22: 311–20.
10. Nugent M, Miller N, Kerin MJ. MicroRNAs in colorectal cancer: function, dysregulation and potential as novel biomarkers. *Eur J Surg Oncol*. 2011; 37: 649–54.

11. Xuan Y, Yang H, Zhao L, Lau WB, Lau B, Ren N, Hu Y, Yi T, Zhao X, Zhou S, Wei Y. MicroRNAs in colorectal cancer: small molecules with big functions. *Cancer Lett*. 2015; 360:89–105.
12. Iorio MV, Visone R, Di Leva G, Donati V, Petrocca F, Casalini P, Taccioli C, Volinia S, Liu CG, Alder H, Calin GA, Menard S, Croce CM. MicroRNA signatures in human ovarian cancer. *Cancer Res*. 2007; 67: 8699–707.
13. Yuan Y, Shen Y, Xue L, Fan H. miR-140 suppresses tumor growth and metastasis of non-small cell lung cancer by targeting insulin-like growth factor 1 receptor. *PLoS One* 2013;8:e73604.
14. Li W, He F. Monocyte to macrophage differentiation-associated (MMD) targeted by miR-140-5p regulates tumor growth in non-small cell lung cancer. *Biochem Biophys Res Commun*. 2014; 450: 844–50.
15. Song B, Wang Y, Xi Y, Kudo K, Bruheim S, Botchkina GI, Gavin E, Wan Y, Formentini A, Kornmann M, Fodstad O, Ju J. Mechanism of chemoresistance mediated by miR-140 in human osteosarcoma and colon cancer cells. *Oncogene*. 2009; 28: 4065–74.
16. Zhai H, Fesler A, Ba Y, Wu S, Ju J. Inhibition of colorectal cancer stem cell survival and invasive potential by hsa-miR-140-5p mediated suppression of Smad2 and autophagy. *Oncotarget*. 2015; 6:19735–46. <https://doi.org/10.18632/oncotarget.3771>.
17. Yang H, Fang F, Chang R, Yang L. MicroRNA-140-5p suppresses tumor growth and metastasis by targeting transforming growth factor beta receptor 1 and fibroblast growth factor 9 in hepatocellular carcinoma. *Hepatology*. 2013; 58: 205–17.
18. Zhang Y, Eades G, Yao Y, Li Q, Zhou Q. Estrogen receptor alpha signaling regulates breast tumor-initiating cells by down-regulating miR-140 which targets the transcription factor SOX2. *J Biol Chem*. 2012; 287: 41514–22.
19. Li W, Jiang G, Zhou J, Wang H, Gong Z, Zhang Z, Min K, Zhu H, Tan Y. Down-regulation of miR-140 induces EMT and promotes invasion by targeting Slug in esophageal cancer. *Cell Physiol Biochem*. 2014; 34: 1466–76.
20. Sand M, Skrygan M, Sand D, Georgas D, Hahn SA, Gambichler T, Altmeyer P, Bechara FG. Expression of microRNAs in basal cell carcinoma. *Br J Dermatol*. 2012; 167: 847–55.
21. Malzkorn B, Wolter M, Liesenberg F, Grzendowski M, Stuhler K, Meyer HE, Reifenberger G. Identification and functional characterization of microRNAs involved in the malignant progression of gliomas. *Brain Pathol*. 2010; 20: 539–50.
22. Tardif G, Hum D, Pelletier JP, Duval N, Martel-Pelletier J. Regulation of the IGFBP-5 and MMP-13 genes by the microRNAs miR-140 and miR-27a in human osteoarthritic chondrocytes. *BMC Musculoskelet Disord* 2009;10:148.
23. Shersher DD, Vercillo MS, Fhied C, Basu S, Rouhi O, Mahon B, Coon JS, Warren WH, Faber LP, Hong E, Bonomi P, Liptay MJ, Borgia JA. Biomarkers of the insulin-like growth factor pathway predict progression and outcome in lung cancer. *Ann Thorac Surg* 2011;92:1805-11; discussion 1811.
24. Ahn BY, Elwi AN, Lee B, Trinh DL, Klimowicz AC, Yau A, Chan JA, Magliocco A, Kim SW. Genetic screen identifies insulin-like growth factor binding protein 5 as a modulator of tamoxifen resistance in breast cancer. *Cancer Res*. 2010; 70: 3013–9.
25. Xiao S, Chang RM, Yang MY, Lei X, Liu X, Gao WB, Xiao JL, Yang LY. Actin-like 6A predicts poor prognosis of hepatocellular carcinoma and promotes metastasis and epithelial-mesenchymal transition. *Hepatology*. 2016; 63: 1256–1271.
26. Ventura A, Jacks T. MicroRNAs and cancer: short RNAs go a long way. *Cell*. 2009; 136: 586–91.
27. Mendell JT. MicroRNAs: critical regulators of development, cellular physiology and malignancy. *Cell Cycle*. 2005; 4: 1179–84.
28. Dong Y, Yu J, Ng SS. MicroRNA dysregulation as a prognostic biomarker in colorectal cancer. *Cancer Manag Res*. 2014; 6: 405–22.
29. Zhang W, Zou C, Pan L, Xu Y, Qi W, Ma G, Hou Y, Jiang P. MicroRNA-140-5p inhibits the progression of colorectal cancer by targeting VEGFA. *Cell Physiol Biochem*. 2015; 37: 1123–33.